Available online at www.sciencedirect.com
SCIENCE DIRECT®

Journal of the European Ceramic Society 24 (2004) 2537–2546
www.elsevier.com/locate/jeurceramsoc

Microstructure and electrical properties of $ZnO–ZrO_2–Bi_2O_3–M_3O_4$ (M=Co, Mn) varistors

Chul-Hong Kim, Jin-Ho Kim*

Department of Inorganic Materials Engineering, Kyungpook National University, Daegu 702-701, South Korea

Received 10 March 2003; received in revised form 14 July 2003; accepted 19 July 2003

Abstract

Phase evolution, microstructure and the electrical properties of ZrO_2-added pyrochlore-free $ZnO–Bi_2O_3–M_3O_4$ (M=Co, Mn) varistors have been studied as functions of ZrO_2 content up to 10 vol% and the sintering temperature between 900 and 1300 °C. Zirconia remained as intergranular second phase particles up to 1100 °C, which retarded densification and inhibited the grain growth of ZnO. At higher temperatures, on the contrary, ZrO_2 particles began to be entrapped in ZnO grains and irreversibly transform from monoclinic to stable cubic phase dissolving transition metal ions. The grain size of ZnO decreased with increasing ZrO_2 content, and increased with the increase of the sintering temperature. Accordingly breakdown voltage changed with both ZrO_2 content and the sintering temperature as was expected. Nonlinear coefficient (α) depended primarily on the sintering temperature: it increased to >40 up to 1000 °C, and significantly decreased to <30 at higher temperatures probably due to the volatilization of Bi_2O_3. While the specimens sintered at 1200 °C or above had relatively high leakage current (I_L) and large clamping ratio (C_R), those with ZrO_2 content of 0.5–5.0 vol% and sintered below 1200 °C revealed low I_L of $\leqslant 20\ \mu A/cm^2$ and C_R well below 2.0. In spite that varistor characteristics of ZrO_2-added system could not match those of commercial ZnO varistors, its low temperature sinterability and ease of breakdown voltage control via ZrO_2 content without a serious loss of its figures of merit are worth noticing, particularly for multi-layered chip varistor (MLV) application.

Keywords: Electrical properties; Grain size; Varistors; ZnO; ZrO_2 addition

1. Introduction

Since it was reported by Matsuoka[1] in the early 1970s that polycrystalline ZnO ceramics incorporated with Sb_2O_3, Bi_2O_3 and several transition metal oxides showed a highly nonohmic conduction, quite many researches and studies have been performed on the fabrication and the physicochemical properties of this material system as well as its device applications for overvoltage protectors and surge absorbers.[2, 3]

The typical ZnO-based system of $ZnO–Sb_2O_3–Bi_2O_3–M_{tr}O$ (M_{tr} = 3d-transition elements) is known to have excellent varistor characteristics: high nonlinear coefficient (α) over 50; low leakage current (I_L) below 10 $\mu A/cm^2$; large surge absorbing capability over 200 J/cm^3. In this system, the reaction sequence and the role of additives are now quite well understood. The key reaction is the following decomposition and recombination of $Zn_2Sb_3Bi_3O_{14}$ pyrochlore on heating and in cooling, respectively, as was suggested by Inada[4]:

$$2Zn_2Sb_3Bi_3O_{14} + 17ZnO \underset{\text{cooling}}{\overset{950–1050^oC}{\rightleftarrows}} 3Zn_7Sb_2O_{12} + 3Bi_2O_3(\ell) \quad (1)$$

Pyrochlore forms below 700 °C on heating by solid state reaction, and reacts with additional ZnO to form grain boundary phases of $Zn_7Sb_2O_{12}$ spinel particles and Bi-rich liquid at ~1000 °C. The former acting as a second phase inhibits rapid grain growth of ZnO, while the latter promotes densification and the grain growth of ZnO.[5] In the meantime, transition metal ions having dissolved to ZnO and pyrochlore redistribute among ZnO grains and the grain boundary phases, and the chemical and microstructural homogeneities attain in high temperature sintering of the ceramic system.[6] In

* Corresponding author. Tel.: +82-53-950-5637; fax: +82-53-950-5645.
E-mail address: jihkim@bh.knu.ac.kr (J.-H. Kim).

0955-2219/$ - see front matter © 2003 Elsevier Ltd. All rights reserved.
doi:10.1016/j.jeurceramsoc.2003.07.002

furnace-cooling of this system, pyrochlore recombines in part according to Eq. (1), and exists along with spinel phase as nonconductive discrete intergranular particles which do not directly influence I–V characteristics of ZnO varistors.

The formation of pyrochlore on heating, however, reduces the amount of Bi-rich liquid responsible for an enhanced densification in the initial stage of sintering.[5,7,8] Moreover, the recombination of pyrochlore in cooling reduces intergranular Bi_2O_3 responsible for high nonlinearity of ZnO varistors.[9] Thus both high temperature sintering over 1100 °C and the addition of α-$Zn_7Sb_2O_{12}$ stabilizing elements such as Co and Mn are required to obtain dense and stable ZnO varistors added with Sb_2O_3.[4,7] Several pyrochlore-free systems such as ZnO–Bi_2O_3–$M_{tr}O$,[10] ZnO–Pr_2O_3–$M_{tr}O$[11] and ZnO–V_2O_5–$M_{tr}O$[12] have been proposed for low-temperature sintering or Bi_2O_3-free ZnO varistors. The electrical properties of these varistor systems such as nonlinear coefficient and leakage current, however, could not be comparable with Sb_2O_3-added ones. Above all things, the main disadvantage of these systems is the absence of grain growth inhibiting second phase which is indispensable for the fabrication of high voltage varistors with homogeneous microstructure and controllable breakdown voltage. The addition of a stable second phase to ZnO–Bi_2O_3–$M_{tr}O$ which is non-reactive to both Bi_2O_3 and host ZnO up to the sintering temperature might be one of the solutions to this problem.

We added ZrO_2 which is non-reactive to ZnO[13] as a promising second phase to pyrochlore-free ZnO–Bi_2O_3–M_3O_4 (M=Co, Mn) system, and investigated phase evolution, microstructure and the electrical properties of the varistor system as functions of ZrO_2 content up to 10 vol% and the sintering temperature between 900 and 1300 °C. This paper describes main results and discusses the volumetric effects of ZrO_2 on the grain growth of ZnO and resultant varistor characteristics.

2. Experimental

Reagent grade ($\geqslant$99.5%) powders of ZnO, α-Bi_2O_3, monoclinic ZrO_2, Co_3O_4 and Mn_3O_4 were used as starting materials. Compositions of ZnO varistors were summarized in Table 1. In each batch mixture the amounts of the respective oxide additives except ZrO_2 were kept 1 at.%; those of ZrO_2 added to balance oxides were 0, 0.5, 1.0, 2.0, 5.0 and 10.0 vol%, of which batches were abbreviated as Z0, Z1, Z2, Z3, Z4 and Z5, respectively. Powder mixtures were calcined at 700 °C, pulverized and uniaxially pressed under 10 MPa into disks of 15 mm in diameter and 3 mm thick, and then CIPed under 150 MPa. Sintering was conducted between 800 and 1300 °C for 1 h.

Densification was studied with linear shrinkage at constant rate heating of 10 °C/min as well as the fired density measured by Archimedes method. Phase evolution during sintering was studied with an X-ray diffractometer (M03-XHF, MacScience) using CuK_α radiation, and microstructure was observed on polished and chemically etched disk sections with a SEM (JSM-5400, Jeol).

With fired disks lapped to 1.0±0.05 mm thick and silvered on opposite sides, I–V characteristics and 8/20 μs impulse current response were examined with an I–V meter (Keithley 237, Keithley) and a pulse generator (E504A, ECAT Keytek) incorporated with an oscilloscope, respectively. C–V characteristics were determined with an impedance gain/phase analyzer (HP4194, Hewlett Packard).

Breakdown voltage (V_{bk}) was determined on I–V curve at the current density of 0.5 mA/cm^2, and then leakage current (I_L) was read on $0.8V_{bk}$. Nonlinear coefficient (α) was calculated using the voltages V_1 and V_2 on I–V curve at 1.0 and 10 mA/cm^2, respectively, according the following equation:

$$\alpha = \log(I_2/I_1)/\log(V_2/V_1) \tag{2}$$

Capacitance (C) of the specimens was measured as a function of dc bias voltage (V), and donor density (N_D) was determined from the slope of $(1/C-1/C_0)^2$ versus V graph according to the following equation:[14]

$$\left(\frac{1}{C}-\frac{1}{2C_0}\right)^2 = \frac{2t}{A^2\overline{d}e\varepsilon N_D}V + \frac{2t^2}{A^2\overline{d}^2e\varepsilon N_D}\phi_b \tag{3}$$

where C_0 and C are the capacitances per unit area of a grain boundary without and with dc bias, respectively, t the thickness of the specimens and A the electrode area of specimen, $\overline{d}$ the average grain and ε the permittivity of ZnO, and e is electron charge. ϕ_b corresponds to double-Schottky potential barrier height on the grain boundaries.

Clamping voltage (V_C) was measured by applying 8/20 μs impulse current with a peak height of 150 A/cm^2, and clamping ratio (C_R) was defined as the ratio of V_C to V_{bk}.

Table 1
Compositions and the abbreviations of ZrO_2-added ZnO varistors

Sample name	ZrO_2 (vol%)	ZnO + Bi_2O_3 + Mn_3O_4 + Co_3O_4 (mol%)
Z0	0.0	98.84 + 0.50 + 0.33 + 0.33 = 100
Z1	0.5	98.84 + 0.50 + 0.33 + 0.33 = 100
Z2	1.0	98.84 + 0.50 + 0.33 + 0.33 = 100
Z3	2.0	98.84 + 0.50 + 0.33 + 0.33 = 100
Z4	5.0	98.84 + 0.50 + 0.33 + 0.33 = 100
Z5	10.0	98.84 + 0.50 + 0.33 + 0.33 = 100

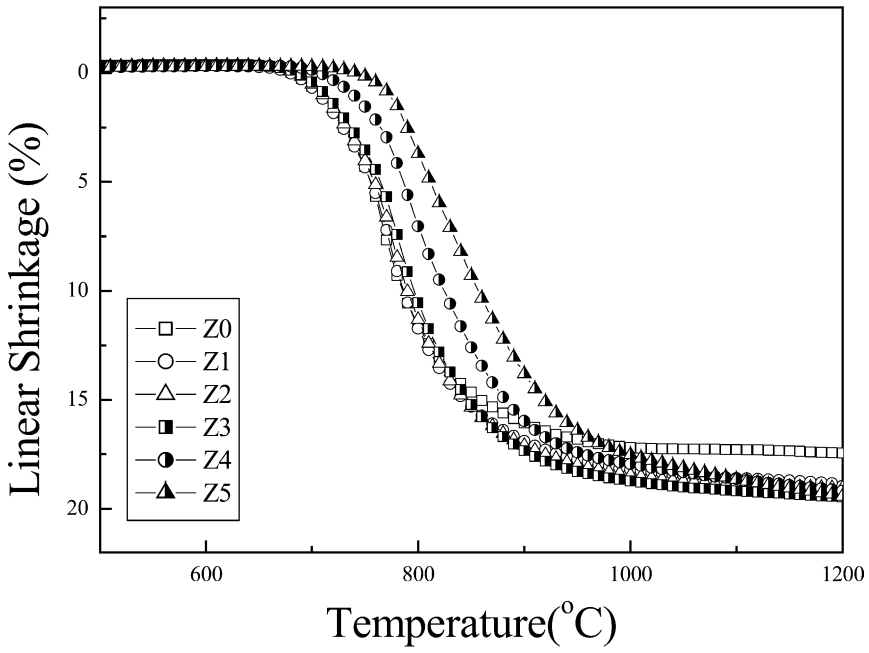

Fig. 1. Linear shrinkages of the specimens on constant-rate heating of 10 °C/min.

3. Results and discussion

3.1. Densification

Fig. 1 shows the linear shrinkages of the specimens on constant-rate heating of 10 °C/min. In powder compact without ZrO_2 (Z0), shrinkage started at ~700 °C, and was completed at ~930 °C. With increasing ZrO_2 content, both the onset and the completion of densification gradually shifted to higher temperatures; in Z3 (2 vol% ZrO_2), those temperatures were ~720 and ~1050 °C; in Z5 (10 vol% ZrO_2), those were ~750 and >1200 °C. Zirconia added to ZnO–Bi_2O_3–M_3O_4 (M=Co, Mn) seems to retard densification as Sb_2O_3 does in the same system[6,13] but quite different mechanisms should be involved in the two systems, which will be discussed later in relation to phase evolution on heating.

Fig. 2 shows the effect of ZrO_2 volume fraction on the fired density of the specimens soaked for 1 h between 800 and 1300 °C. Relative density at 800 °C decreased with increasing amount of ZrO_2 in correspondence with the result shown in Fig. 1. At 900 °C, however, all the specimens attained saturated densities over 96% regardless of the amount of ZrO_2 in 1 h-soaking, which could not ever be attained in ZnO–Sb_2O_3–Bi_2O_3 system.[5] Above 1000 °C, the relative density gradually decreased with increasing sintering temperature, probably due to pore growth and the volatilization of liquid Bi_2O_3.[6,15]

3.2. Phase evolution

Fig. 3 illustrates XRD profiles of Z0 and Z4 sintered between 800 and 1300 °C for 1 h. Throughout the temperature range studied there were no fundamental differences in the phase evolution between Z0 and ZrO_2-added ones except the existing ZrO_2 and its phase change in the latter: $ZnBi_{38}O_{60}$ which enables rapid densification via particle rearrangement in eutectic melting[6] appeared at 800 °C; in 900 °C or higher temperatures sintering specimens, mixed phases of α- and β-Bi_2O_3 appeared by the solidification of Bi-rich liquid phase regardless of the amount of ZrO_2 added; part of monoclinic ZrO_2 transformed to cubic phase above 1100 °C presumably by dissolving co-added transition metal oxides. Even if clear diffraction peaks of ZrO_2 did not appear in both Z1 and Z2 due to the resolution limit of XRD, it is believed that ZrO_2 neither reacted with nor dissolved to host ZnO but remained as second phase throughout the sintering process. Furthermore, the polymorphism of Bi_2O_3 in ZrO_2-added system seemed not to be influenced by the cooling rate from 2 °C/min up to water quenching, which is different from Sb_2O_3-added ZnO varistors.[16] As long as the chemical reaction is concerned, ZrO_2 is thought a promising candidate for inert second phase of ZnO varistors keeping the state of Bi_2O_3 unaffected throughout the sintering procedure.

3.3. Microstructure development

Fig. 4 illustrates SEM images of the specimens sintered between 1000 and 1200 °C, and the grain size data of ZnO are presented as a function of sintering temperature in Fig. 5. Two-phase microstructure is seen in Z0 consisting of large ZnO grains entrapping many micropores and intergranular Bi_2O_3, typical of rapid

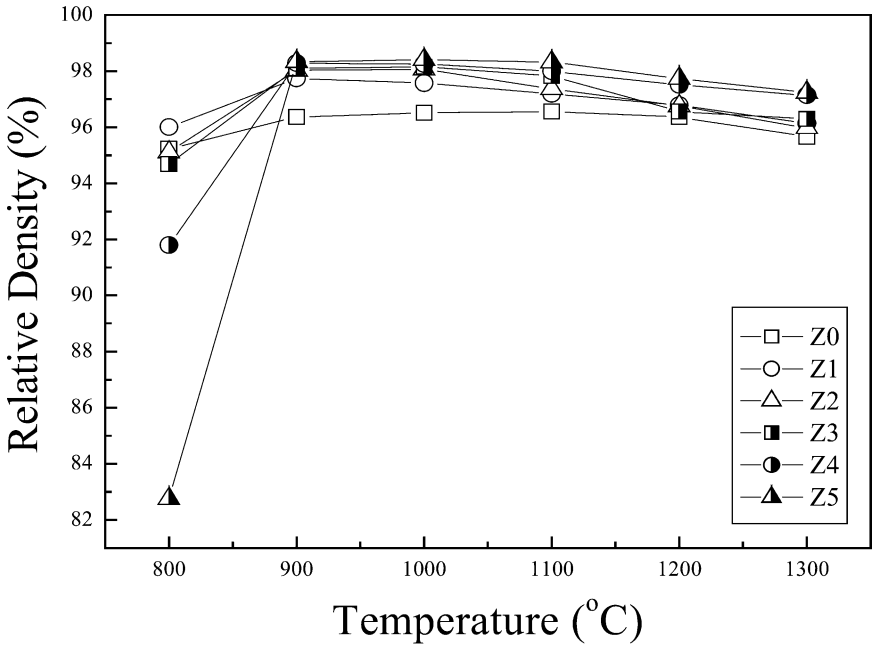

Fig. 2. Change in the relative density of the specimens with sintering temperature.

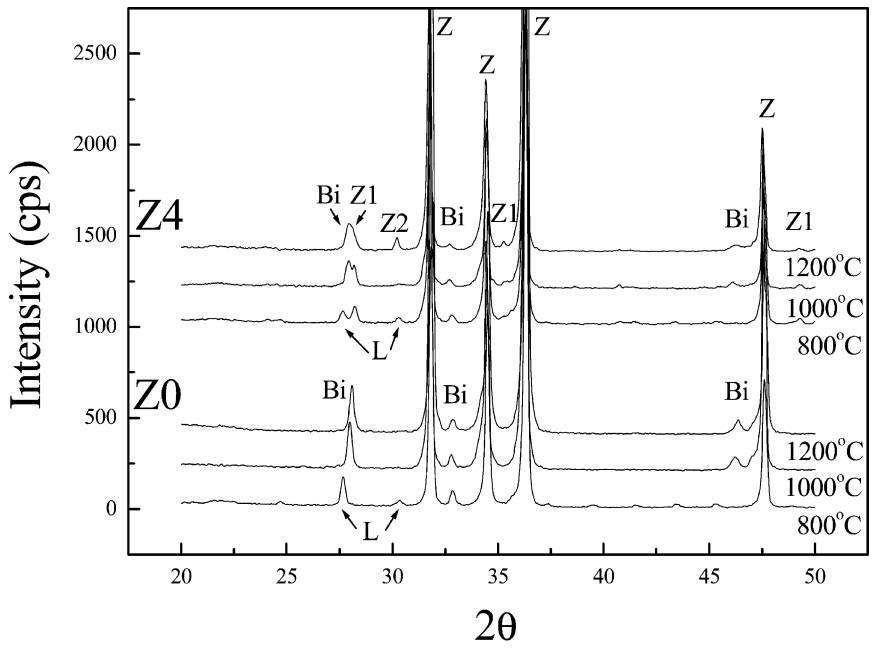

Fig. 3. XRD profiles of Z0 and Z4 sintered between 800 and 1200 °C for 1 h. (Z: ZnO, L: $ZnBi_{38}O_{60}$, Bi: α- and β-Bi_2O_3, Z1: monoclinic-ZrO_2, Z2: cubic-ZrO_2).

grain growth in liquid phase sintering. ZrO_2-added specimens Z1, Z3 and Z5, on the other hand, are composed of three phases as was confirmed by XRD (See Fig. 3): host ZnO grains; fine spherical ZrO_2 particles as second phase; Bi_2O_3 films solidified on the grain boundaries and corners in cooling. In ZrO_2-added specimens sintered at 1000 °C, practically no pores are observed in ZnO grains, and most ZrO_2 particles are located at grain junctions. In those specimens sintered at 1200 °C, however, both micropores and spherical ZrO_2 particles exist within ZnO grains as well as on grain corners and boundaries. The grain size of ZnO increased with the increase of sintering temperature, and decreased with increasing ZrO_2 content throughout the sintering temperature range studied. Microstructure of Z1, however, becomes very similar to that of Z0 in 1200 °C sintering.

It is well known that Zener drag intensifies with the volumetric increase and/or particle size reduction of

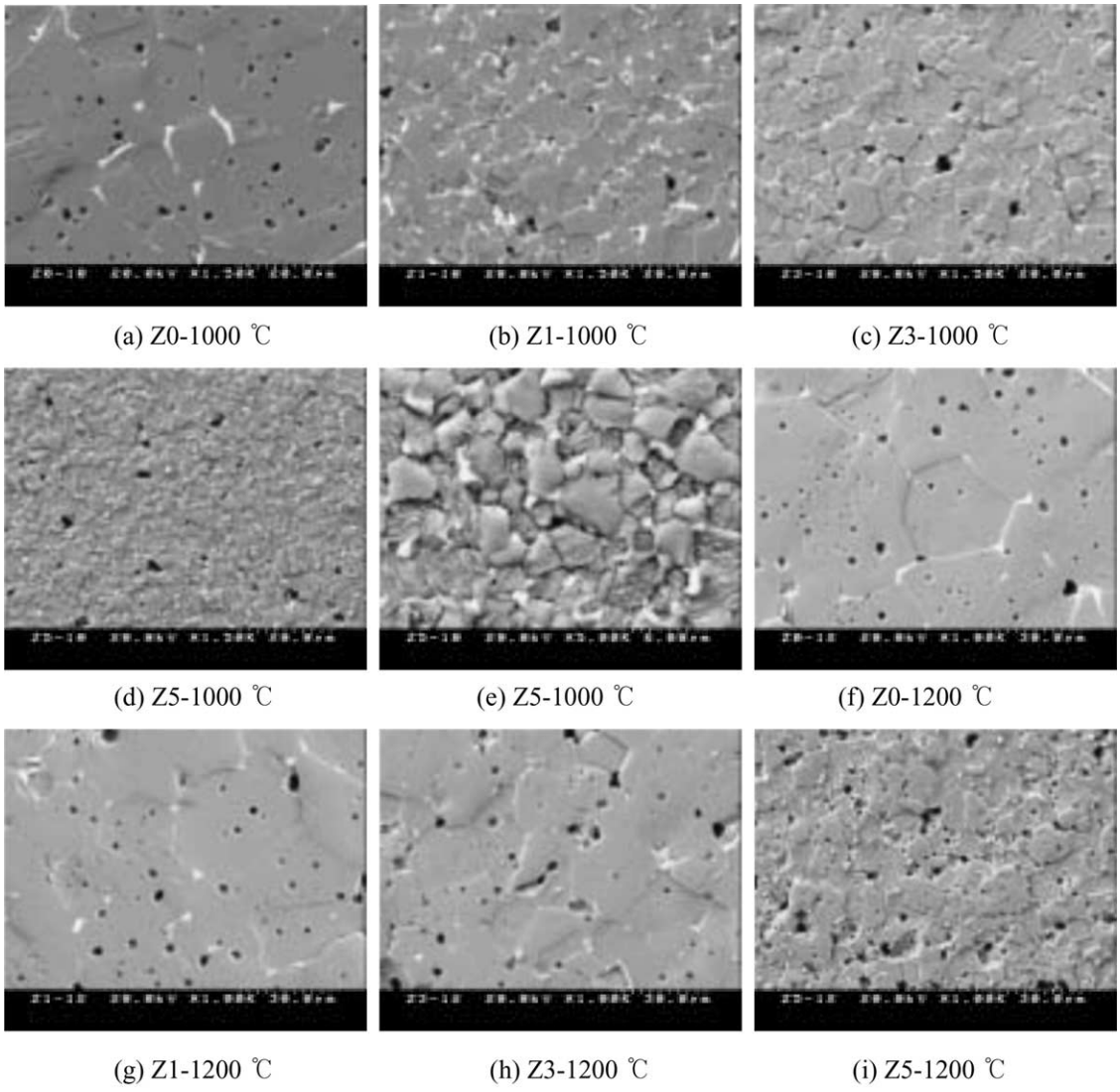

Fig. 4. SEM photographs (BEI images) of the specimens sintered at (a)–(e): 1000 °C and (f)–(i): 1200 °C for 1 h, (e) is a magnified image of (d).

second phase.[17] In the present study, the Zener effect of ZrO_2 particles on the grain boundary movement is thought responsible for inhibited grain growth of ZnO. According to rough calculation using theoretical densities and molecular weights of $Zn_7Sb_2O_{12}$ and ZnO, x mol% Sb_2O_3 added to ZnO change to $\sim 10x$ vol% $Zn_7Sb_2O_{12}$ in Sb_2O_3-containing ZnO varistors. Thus the amounts of ZrO_2 as second phase in Z1, Z3 and Z5 are comparable with those of $Zn_7Sb_2O_{12}$ in ZnO doped with 0.05, 0.2 and 1.0 mol% Sb_2O_3, respectively. Grain size of Z5, however, is much smaller than that of corresponding ZnO–Sb_2O_3–Bi_2O_3 previously reported.[5] It is reasonable that much smaller size of ZrO_2 particles as shown in Fig. 4 compared with spinel particles in conventional varistors resulted in the smaller grain size of ZrO_2-added system. As far as grain growth control is concerned, less than 1.0 vol% ZrO_2 seems insufficient in the sintering of ZnO–Bi_2O_3–M_3O_4.

3.4. I–V characteristics

Fig. 6 shows I–V characteristics of the specimens sintered at 1000 °C. For the sake of comparison, data are presented in electric field (V/cm)—current density (mA/cm^2) relation. It is clearly shown that the breakdown curve shifts to higher electric field region with increasing ZrO_2 content of the specimens.

In Figs. 7–9, breakdown voltage (V_{bk}), nonlinear coefficient (α) and leakage current (I_L) evaluated from the results of I–V measurement are presented as functions of ZrO_2 content and sintering temperature. In the present varistor system, as the chemical properties of the grain boundaries in relation to double Schottky barriers can be regarded as essentially consistent irrespective of the composition, breakdown voltage data are thought primarily related with the grain size data shown in Fig. 5: V_{bk} decreases and ZnO grain size

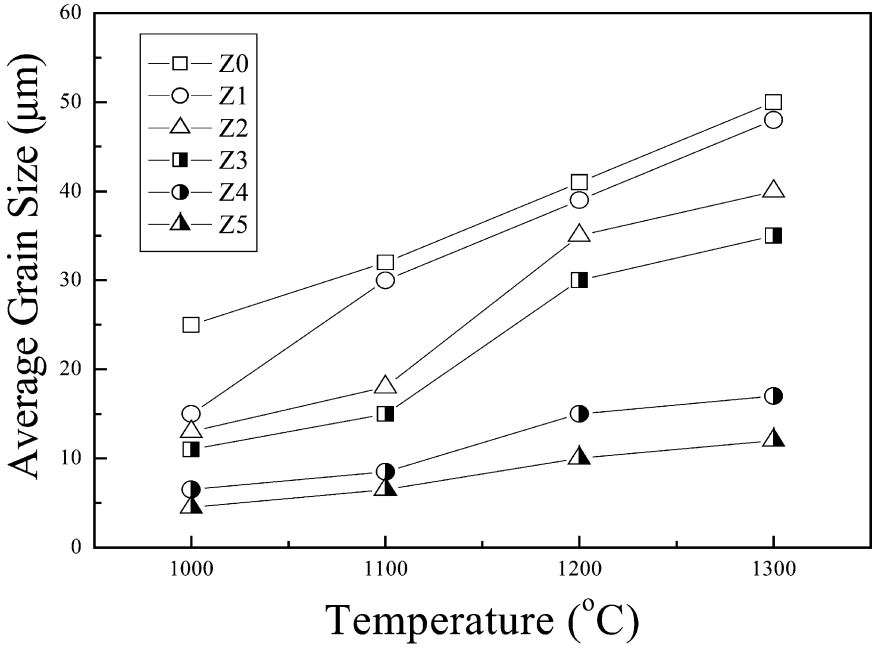

Fig. 5. Grain growth of the specimens as a function of ZrO_2 content and sintering temperature.

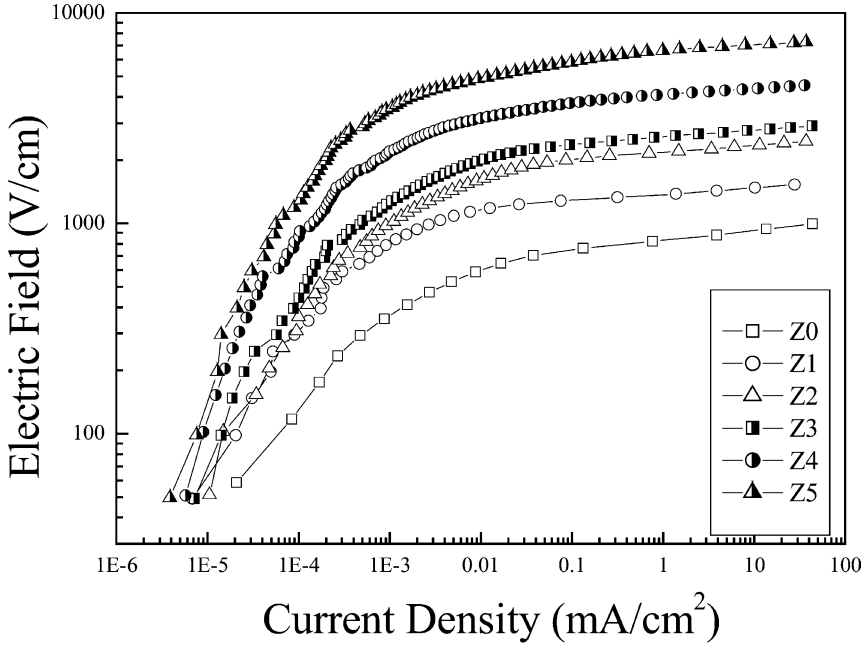

Fig. 6. I–V characteristics of ZrO_2-added ZnO varistors sintered at 1000 °C.

increases with the increase of sintering temperature in each composition; throughout the sintering temperature range V_{bk} increases monotonically with the increase of ZrO_2 content, while the rate of change increases with the increase of ZrO_2 content. Nonlinear coefficient (α) also increases with increasing ZrO_2 content but is strongly dependent on sintering temperature: at 900 °C, the specimens with more than 2.0 vol% ZrO_2 does not show a breakdown up to 10^4 V/cm, probably due to their fine-grained structures; in all the specimens α increases up to 1000 °C (25 in Z0 and 52 in Z5) and then significantly decreases at higher temperatures (12 in Z0 and 30 in Z5 at 1200 °C). In each sintering temperature, leakage current (I_L) becomes minimized well below 10 $\mu A/cm^2$ at a certain composition and then gradually increases with increasing ZrO_2 content. Furthermore, the composition rendering minimum I_L shifts to higher ZrO_2 content with the increase of sintering temperature. While all the specimens sintered at 1200 °C or above reveal relatively high I_L over 20 $\mu A/cm^2$, those sintered

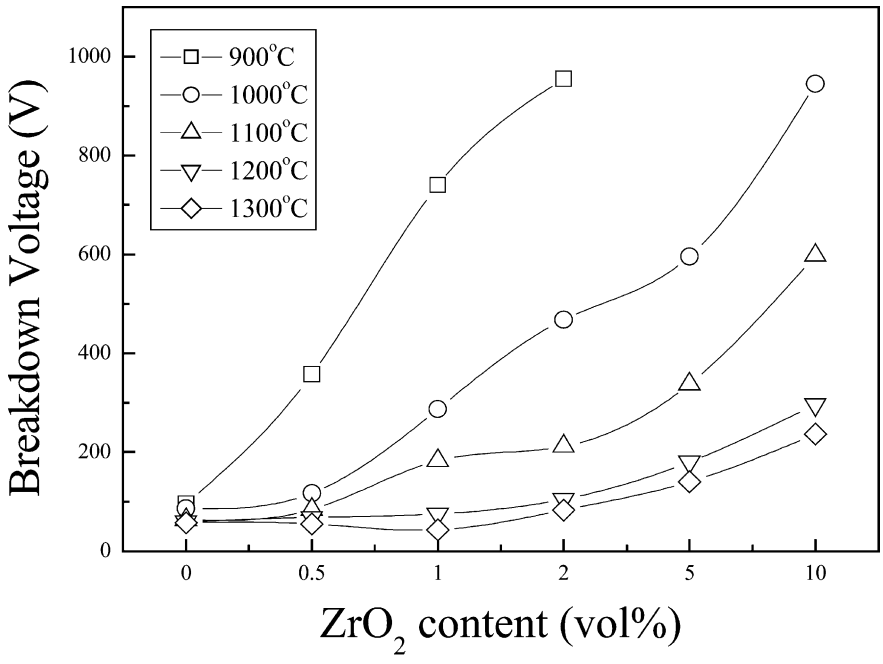

Fig. 7. Breakdown voltage (V_{bk}) of ZrO_2-added ZnO varistors as a function of ZrO_2 content and sintering temperature, estimated at the current density of 0.5 mA/cm^2.

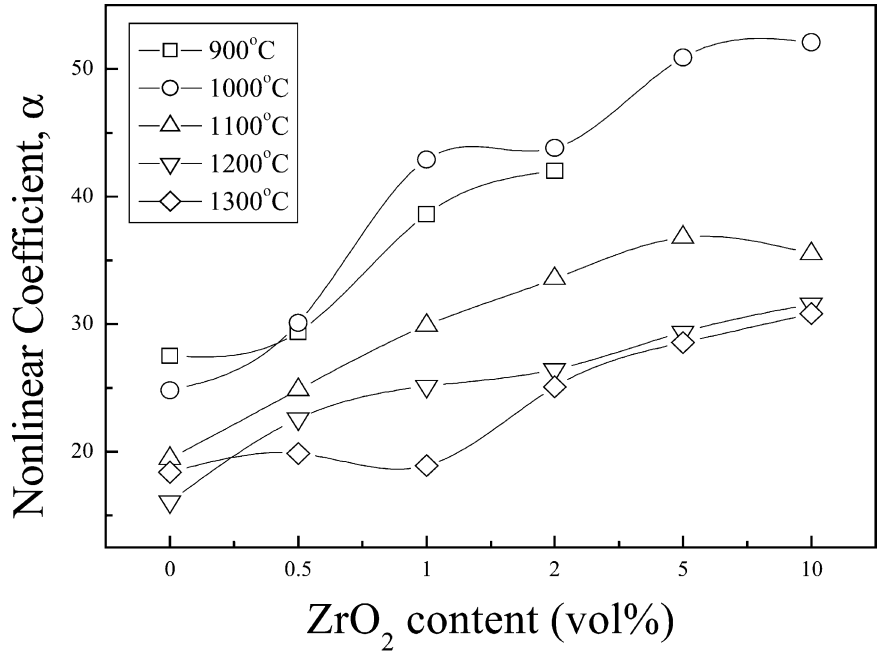

Fig. 8. Nonlinear coefficient (α) of ZrO_2-added ZnO varistors as a function of ZrO_2 content and sintering temperature.

below 1100 °C with ZrO_2 content of 0.5–5.0 vol% have quite low I_L of $\leqslant 10$ μA/cm^2.

It is believed that the enhancement of varistor characteristics in ZrO_2-added specimens stems from the controlling effect of second phase ZrO_2 on the grain growth of ZnO, which enables more homogeneous microstructure particularly at low sintering temperatures below 1200 °C. Different from Z0 which had no second phase particles, of ZrO_2-added ones revealed controlled varistor characteristics simply by adjusting the sintering condition and ZrO_2 content as expected. The mechanism of thorough degenerations of varistor characteristics in high-temperature sintering specimens, however, has not been clarified yet. At present, the volatilization of Bi_2O_3 is thought influential mechanism as in the case of the density decrease. The reaction

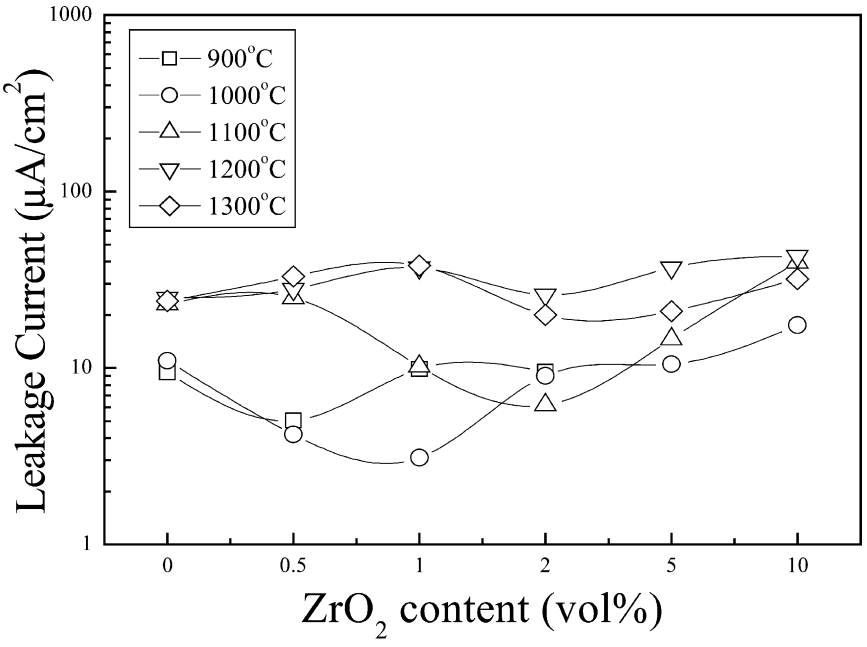

Fig. 9. Leakage current (I_L) of ZrO_2-added ZnO varistors as a function of ZrO_2 content and sintering temperature, estimated at 0.8 V_{bk}.

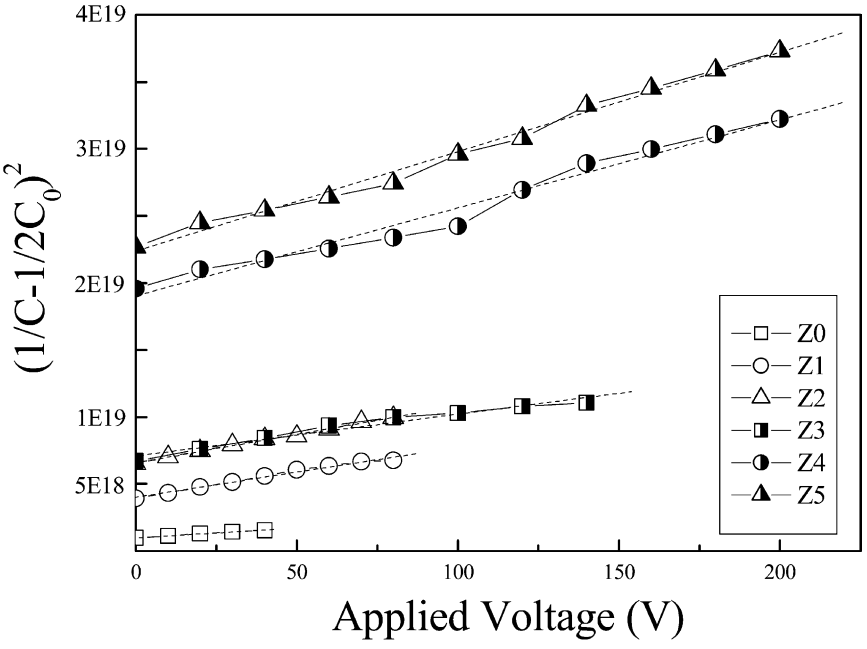

Fig. 10. Capacitance–voltage (C–V) characteristics of ZrO_2-added ZnO varistors sintered at 1100 °C.

between ZrO_2 and the other constituents above 1100 °C as shown in Fig. 3 might have an undesirable influence on the characteristics of double Schottky barrier.

3.5. C–V and current impulse response

Fig. 10 shows capacitance-voltage (C–V) characteristics of ZrO_2-added ZnO varistors sintered at 1100 °C, and donor density (N_D) calculated from the slopes of the lines in Fig. 10 as well as capacitance (C_0) are presented in Fig. 11. With increasing ZrO_2 content, capacitance decreased from 50 pF of Z0 to 10 pF of Z5 while donor density remained essentially unchanged at $\sim 1\times10^{17}/cm^3$. It is believed that ZrO_2 added to the system did not affect N_D of ZnO grains due to its non-reactivity with ZnO. As the same N_D theoretically ensures the same equilibrium thickness of depletion layers which act as dielectric media between a pair of semi-conductive ZnO grains in ZnO-based barrier-layer capacitor, it is plausible that decrease of grain size with the increase of ZrO_2 content is responsible for the capacitance decrease.[18] Donor density calculated in the

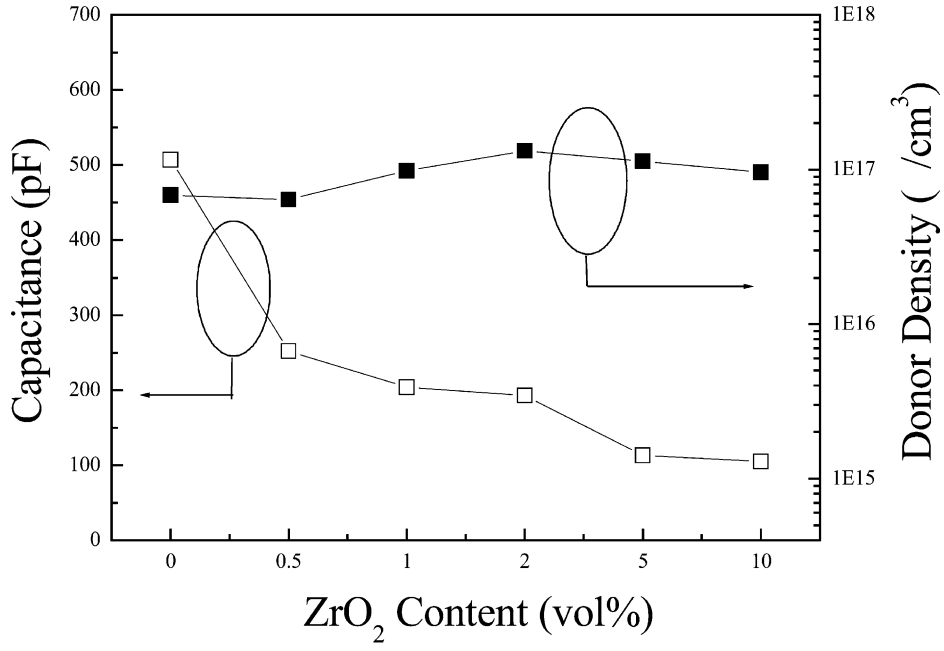

Fig. 11. Capacitance (C_0) and donor density (N_D) of ZrO_2-added ZnO varistors sintered at 1100 °C, calculated with C–V measurement data.

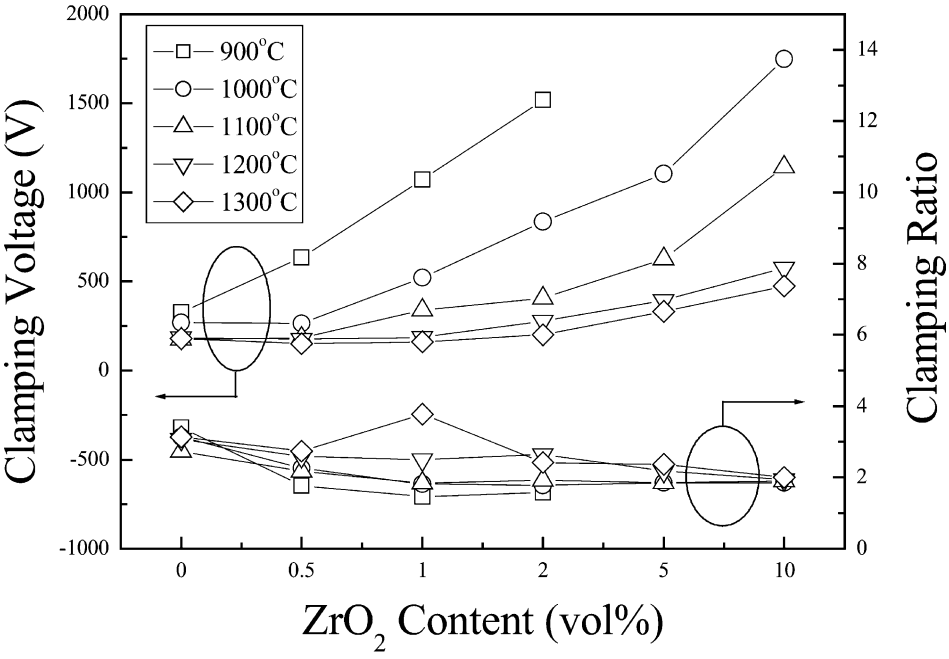

Fig. 12. Clamping voltage (V_C) and clamping ratio (C_R) of ZrO_2-added ZnO varistors as a function of ZrO_2 content and sintering temperature.

present study was about one order of magnitude smaller than those of various commercial-grade ZnO varistor systems. The development of active donor dopants including their concentrative optimization in ZrO_2-added ZnO varistor system is presently being performed.

Fig. 12 shows the effects of ZrO_2 addition on clamping voltage (V_C) and clamping ratio (C_R) reflecting upturn I–V characteristics of the specimens. The tendency of V_C change with ZrO_2 content and sintering temperature seems very similar to that of V_{bk} shown in Fig. 7, which implies the primary dependence of V_C on the grain size of ZnO. Clamping ratio (C_R), regarded as the criterion of surge handling ability of surge absorbing devices, kept well below 2.0 in ZrO_2-added and 1100 °C or lower temperatures sintering specimens but was apt to increase with higher temperatures sintering. As the closer C_R to unity represents the higher surge handling ability,[19,20] it can be said that sintering ZrO_2-added ZnO varistors below 1200 °C is more beneficial for surge handling applications. There has been no fundamental

difference of C_R values among the specimens with varying ZrO_2 content, and the typical value of ~1.8 of the present study is somewhat larger than that of 1.4–1.6 of ZnO–Sb_2O_3–Bi_2O_3–$M_{tr}O$.[20]

On the whole, varistor characteristics of the present ZrO_2-added system do not match those of commercial ZnO–Sb_2O_3–Bi_2O_3–$M_{tr}O$.[21] None the less, the low temperature sinterability and ease of breakdown voltage control via ZrO_2 content without a significant loss of figs. of merit are worth noticing, particularly in MLV application. Further research on the grain boundary characteristics and the electrical degradation mechanism are presently being performed.

4. Conclusions

Pyrochlore-free, microstructure controllable ZnO–Bi_2O_3–M_3O_4 (M=Co, Mn) varistors have been obtained with the addition of ZrO_2 up to 10 vol%. Up to the sintering temperature of 1100 °C, ZrO_2 remained as chemically stable second phase particles among ZnO grains, and thus retarded densification and inhibited the grain growth of ZnO in the liquid phase sintering. Above 1100 °C, however, irreversible monocliniccubic phase transition of ZrO_2 proceeded with the dissolution of Co and Mn, and part of ZrO_2 particles as well as micropores were entrapped in ZnO grains.

Grain growth of ZnO could be effectively controlled by adjusting ZrO_2 content and sintering temperature up to 1100 °C, which enabled a wide-range adjustment of varistor breakdown voltage without significant deteriorations of other varistor characteristics such as nonlinear coefficient (α), leakage current (I_L) and clamping ratio (C_R) compared with commercial Sb_2O_3-containing ZnO varistors: α over 30; I_L not exceeding 20 $\mu A/cm^2$; C_R below 2.0. Sintering over 1100 °C, in contrast, resulted in poor varistor characteristics, probably due to density decrease by pore growth and increased volatilization of liquid Bi_2O_3. In addition, both of the compositions with ZrO_2 contents of 0.5 and 10 vol% did not satisfy the requirements of grain growth control and low temperature sintering of ZnO-based varistors due to their inadequate Zener effects, respectively.

The current results suggest that the low temperature sinterability and ease of breakdown voltage control via ZrO_2 content without a significant loss of figures of merit of ZnO varistors are worth noticing particularly in MLV application.

Acknowledgements

Lattron Co., LTD. (Daejeon, Republic of Korea) is acknowledged for their financial support and materials supply. We would like to thank Dr. C. K. Lee for his valuable comments and suggestions.

References

1. Matsuoka, M., Nonohmic properties of zinc oxide ceramics. *Jpn. J. Appl. Phys*, 1971, **10**, 736–746.
2. Gupta, T. K., Application of zinc oxide varistors. *J. Am. Ceram. Soc.*, 1990, **73**, 1817–1840.
3. Clarke, D. R., Varistor ceramics. *J. Am. Ceram. Soc.*, 1999, **82**, 485–502.
4. Inada, M., Formation mechanism of nonohmic zinc oxide ceramics. *Jpn. J. Appl. Phys*, 1980, **19**, 409–419.
5. Kim, J.-H., Kimura, T. and Yamaguchi, T., Sintering of zinc oxide doped with antimony oxide and bismuth oxide. *J. Am. Ceram. Soc.*, 1989, **72**, 1390–1395.
6. Hong, Y.-W. and Kim, J.-H., Phase formation and the sintering behavior of Mn-doped ZnO–Bi_2O_3–Sb_2O_3 varistor system. *J. Kor. Ceram. Soc.*, 2000, **37**, 651–659 (in Korean)..
7. Leite, E. R., Nobre, M. A., Longo, E. and Varela, J. A., Microstructural development of ZnO varistor during reactive liquid phase sintering. *J. Mater. Sci.*, 1996, **31**, 5391–5398.
8. Mergen, A. and Lee, W. E., Microstructural relations in BZS pyrochlore-ZnO mixtures. *J. Eur. Ceram. Soc.*, 1997, **17**, 1049–1060.
9. Eda, K., Conduction mechanism of non-ohmic zinc oxide ceramics. *J. Appl. Phys.*, 1978, **49**, 2964–2972.
10. Ezhilvalavan, S. and Kutty, T. R. N., Dependence of non-linearity coefficients on transition metal oxide concentration in simplified compositions of ZnO + Bi_2O_3 + MO varistor ceramics (M=Co or Mn). *J. Mater. Sci.: Mater. in Electr.*, 1996, **7**, 137–148.
11. Mukae, K., Tsuda, K. and Nagasawa, I., Non-ohmic properties of ZnO rare earth metal oxide-Co_3O_4 ceramics. *Jpn. J. Appl. Phys*, 1977, **16**, 1361–1368.
12. Tsai, J. K. and Wu, T. B., Microstructure and nonohmic properties of ZnO–V_2O_5 ceramics. *Jpn. J. Appl. Phys*, 1995, **34**, 6452–6457.
13. Fan, C. L. and Rahaman, M. N., Factors controlling the sintering of ceramic particulate composites: I, conventional processing. *J. Am. Ceram. Soc.*, 1992, **75**, 2056–2065.
14. Mukae, K., Tsuda, K. and Nagasawa, I., Capacitance-vs-voltage characteristics of ZnO varistors. *J. Appl. Phys.*, 1977, **50**, 4475–4476.
15. Kim, C.-H. and Kim, J.-H., Sintering and the electrical properties of Co-doped ZnO–Bi_2O_3–Sb_2O_3 varistor system. *J. Kor. Ceram. Soc.*, 2000, **37**, 186–193 (in Korean)..
16. Inada, M., Effects of heat-treatment on crystal phases, microstructure and electrical Properties of nonohmic zinc oxide ceramics. *Jpn. J. Appl. Phys*, 1979, **18**, 1439–1446.
17. Nes, E., Ryum, N. and Hunderi, O., On the Zener drag. *Acta Metall*, 1985, **33**, 11–22.
18. Wernicke, R., Two-layer model explaining the properties of $SrTiO_3$ boundary layer capacitors. In *Grain Boundary Phenomena in Electronic Ceramics*, ed. L. M. Levinson. The American Ceramic Society, Columbus, 1981, pp. 272–281.
19. Kim, C.-H. and Kim, J.-H., Enhanced nonlinearity of a ZnO-based varistor doped with alum ($AlK(SO_4)_2{\cdot}12H_2O$). *Key Eng. Mater.*, 2002, **228-229**, 185–190.
20. Toal, F. J., Dougherty, J. P. and Randall, C. A., Processing and electrical characterization of a varistor-capacitor cofired multilayer device. *J. Am. Ceram. Soc.*, 1998, **81**, 2371–2380.
21. Tokunaga, H., Wakahata, Y. & Mutoh, N., Varistor formed of bismuth and antimony and method of manufacturing same. US Patent 5592140, 7 January 1997.